Mon. Not. R. Astron. Soc. **328,** 520–526 (2001)

Galactosynthesis predictions at high redshift

Ari Buchalter,[1] Raul Jimenez[2★] and Marc Kamionkowski[1]
[1]*California Institute of Technology, Mail Code 130-33, Pasadena, CA 91125, USA*
[2]*Department of Physics and Astronomy, Rutgers University, 136 Frelinghuysen Road, Piscataway, NJ 08854–8019, USA*

Accepted 2001 August 8. Received 2001 August 8; in original form 2001 February 8

ABSTRACT

We predict the Tully–Fisher (TF) and surface-brightness–magnitude relations for disc galaxies at $z = 3$ and discuss the origin of these scaling relations and their scatter. We find that both halo dynamics and the star formation history play important roles, and we show that the variation of the TF relation with redshift can be a potentially powerful discriminator of galaxy-formation models. In particular, the TF relation at high redshift might be used to break parameter degeneracies among galactosynthesis models at $z = 0$, as well as to constrain the redshift distribution of collapsing dark-matter haloes, the star formation history and baryon fraction in the disc and the distribution of halo spins.

Key words: galaxies: formation – galaxies: kinematics and dynamics – galaxies: spiral – cosmology: theory.

1 INTRODUCTION

With the advent of numerous 10-m class telescopes, adaptive optics and high-z galaxy surveys, it is becoming possible to learn about the detailed properties of galaxies at high z. In the future, we may expect improved infrared (IR) sensitivity with the Next Generation Space Telescope (NGST) and 30- or even 100-m telescopes, and this should usher in an era of high-precision kinematic and photometric studies of high-z galaxies. Disc galaxies, which constitute the bulk of the present-day galaxy population, are particularly important to our understanding of galaxy formation and evolution, as they are believed to undergo a relatively smooth formation process, and possibly serve as building blocks in the formation of other galactic systems through mergers.

Many authors have investigated galactosynthesis models, both locally and at high redshift (e.g. Dalcanton, Spergel & Summers 1997; Avila-Reese, Firmani & Hernandez 1998; Jimenez et al. 1998; Mo, Mao & White 1998; Somerville & Primack 1999; van den Bosch 2000; Avila-Reese & Firmani 2000; Firmani & Avila-Reese 2000; Mo & Mao 2000; Navarro & Steinmetz 2000), in which the properties of disc galaxies are determined primarily by the mass, size and angular momenta of the haloes in which they form, and which may contain the effects of supernova feedback, adiabatic disc contraction, cooling, merging and a variety of star formation (SF) recipes. In an earlier paper, we (Buchalter, Jimenez & Kamionkowski 2001, hereafter BJK) investigated a variety of galactosynthesis models with realistic stellar populations and made multiwavelength predictions for the Tully–Fisher (TF) relation. With reasonable values for various cosmological parameters, spin (λ) distributions, formation-redshift (z_f) distributions and no supernova feedback, we could produce an excellent fit to the local TF relation at all investigated wavelengths (B, R, I and K), as well as to B-band TF data at $z = 1$, and to the surface-brightness–magnitude (μ–M) relation locally and at $z = 0.4$. These successes suggest that our simplified approach captures the essential phenomenology, even if it leaves out some of the details of more sophisticated models. Thus, our aim here is not to provide a rigorously complete model for disc-galaxy formation, but rather to gain a more basic understanding of relevant processes by exploring a simplified yet successful model with a relatively minimal set of ingredients.

In this paper, we investigate the high-z TF predictions for our model. We examine the key factors impacting the TF relation at high z, and demonstrate that degeneracies among parameters in galactosynthesis models at $z = 0$ can be disentangled at high z. We find that, in addition to the halo dynamics, the disc SF history plays a critical role in determining the high-z TF relation and its subsequent evolution, owing to a stronger dependence of stellar luminosity on mass and age at early times. Information about the z_f and λ distributions, as well as the disc baryon fraction and SF efficiency, may also be gleaned from the high-z TF relation.

2 THE MODELS

Here, we briefly review the main ingredients of our model, based in turn upon that of Heavens & Jimenez (1999) and refer the interested reader to BJK for a comprehensive description. We use the spherical-collapse model for haloes (Mo et al. 1998), the distribution of halo-formation times from the merger-tree formalism (Lacey & Cole 1993, 1994), and a joint distribution in λ and ν, the peak height (Heavens & Peacock 1988; Catelan & Theuns 1996). Haloes are treated as isothermal spheres with a fixed

★E-mail: raulj@physics.rutgers.edu

baryon fraction and specific angular momentum, and their embedded gaseous discs, assumed to form at virialization, have an exponential density profile.[1] We implicitly assume that the haloes of spiral galaxies form smoothly, rather than from major mergers (BJK; Eisenstein & Loeb 1996). An empirical Schmidt law relates the star formation rate (SFR) to the disc surface density (Kennicutt 1998). A Salpeter initial mass function, a prescription for chemical evolution and a synthetic stellar population code (Jimenez et al. 1998) provide the photometric properties of discs at any z.

The model is defined by cosmological parameters and by the time when the most massive progenitor contains a fraction f of the present-day mass, when a halo is defined to form. We found that excellent agreement with current data was obtained by our 'Model A', a *COBE*-normalized ΛCDM cosmogony with $\Omega_0 = 0.3$, $h = 0.65$, $\Omega_b h^2 = 0.019$, an untilted power spectrum with a shape parameter given by $\Gamma = \Omega_0 h$ (Bardeen et al. 1986; Bunn & White 1997) and with $f = 0.5$. The TF relation in this model relied on both halo properties and the SF history of the disc. The local TF scatter arose primarily from the z_f distribution, and secondarily from chemical evolution and the ν–λ anticorrelation. In this model, disc formation occurs primarily at $0.5 \lesssim z \lesssim 2$, and the TF slope steepens and the zero points get fainter from $z = 0$ to $z = 1$. Moreover, the amount of gas expelled from or poured into a disc galaxy in this model is relatively small and the disc and halo specific angular momenta are equal. The results also demonstrated the importance of multiwavelength constraints in fitting the observed TF relation.

A suite of other models that give good fits to the observations at low z can also be found, however. To illustrate, we examine two alternative models, which, though less observationally favoured, also meet the considerable burden of yielding comparably good fits to the slope, zero-point *and* scatter of the TF relation at $z = 0$ in B, R, I and K. The first is a CDM model with $\Omega_0 = 1$, $h = 0.65$, constant metallicity given by the solar value, $\lambda = 0.05$ for all discs, an untilted power spectrum with amplitude $\sigma_8 = 0.5$ and empirical shape parameter value of $\Gamma = 0.2$, and $f = 0.5$. As shown in BJK and elsewhere, high-Ω_0 models generally produce disc galaxies too faint to lie on the local TF relation. To compensate for this, we assume $\Omega_b h^2 = 0.045$, and thus term this the 'high-Ω_b' model.

Our second alternative is a ΛCDM cosmogony like Model A, but with metallicity held constant at the solar value, $\lambda = 0.05$ for all discs and $f = 0.9$. This results in a narrow distribution of formation times peaked around $z \sim 0.2$ (for L_*-type discs), with appreciable ongoing formation today and almost no haloes forming earlier than $z = 1$ (cf. fig. 1 of BJK). We thus denote this the 'low-z_f' model. This model will produce extremely young and bright discs (cf. fig. 5 of BJK).[2] To compensate for this, we reduce the efficiency of SF in our Schmidt-law prescription by 50 per cent [see equations (2)–(4) in BJK]. This lower SF efficiency may be plausible given the lower disc gas fractions predicted by our Model A as compared with values observed by McGaugh & De Blok (1997; see BJK for details).

The left, middle and right panels of Fig. 1 depict the $z = 0$ predictions for the A, high-Ω_b and low-z_f models, in the B, R, I and K bands, respectively. In each panel, the solid line shows a least-squares fit to the TF relation prediction, with a zero-point and slope given by 'a' and 'b', respectively, and 1σ errors given by the dashed lines and denoted in each plot by 'σ'. The four scattered-dot curves in each plot trace the predicted TF spread for four fixed masses (10^{10}, 10^{11}, 10^{12} and $10^{13}\,\mathrm{M}_\odot$), using ∼120 points each. The open symbols represent extinction-corrected data from Tully et al. (1998), comprising spiral galaxies in the loose clusters of Ursa Major and Pisces. In each plot, the data are fitted to the corresponding model, and the value of p gives the probability of obtaining a value of χ^2 as large as that measured, given that the model is correct. As the data have excluded spirals that show evidence of merger activity or disruption, we exclude those galaxies with $B - R < 0.3$ from our predictions.

Each of the three models yields a reasonable fit to the slope and normalization of the TF relation in all wavebands. Moreover, the predicted scatter in the B, R, I and K bands roughly agrees with the observed values of 0.50, 0.41, 0.40 and 0.41, respectively, with the largest discrepancies occurring in the bluer bands, for reasons discussed in BJK.

It is worth exploring whether our predicted M/L ratios at low redshift are in agreement with modern observations. For example, for haloes with $V_c = 200\,\mathrm{km\,s^{-1}}$, the 1σ range in mag is $-19.5 < M_B < -21.5$ and $-23 < M_K < -24$ (for Model A, Fig. 1). The average redshift of collapse for this V_c is $z \sim 1.5$, therefore using equation (2) of BJK we find that the corresponding halo mass is $1.15 \times 10^{12}\,\mathrm{M}_\odot$ and the disc baryonic mass is $1.57 \times 10^{11}\,\mathrm{M}_\odot$. This translates in average $M/L_{B\odot} = 4.5$ and $M/L_{K\odot} = 0.9$, which are in good agreement with recent determinations of stellar M/L ratios (e.g. Roberts & Haynes 1994; Bottema 1996; Verheijen 1997).

Note that the fact that the formation redshift is not zero plays an important role in lowering the mass of the dark halo. The correct formula for determining the mass of the dark halo for a given V_c is equation (2) of BJK. As the formation redshift of most galaxies in our models is not zero (see fig. 1 of BJK), the masses are smaller than their corresponding counterparts at redshift zero. This is important in order to recover reasonable M/L ratios. This also serves to obtain masses of haloes that are not shifted towards low V_c, despite the fact that in our model $V_c = (2/3)^{0.5} V_{\mathrm{vir}}$, which, in any case, only lowers V_c by a factor of 0.82. It is important to remember that the f parameter in the Lacey & Cole (1993) model is a free parameter in our model that we use to fit the observed TF. In case of Model A, the best value obtained for f was 0.5 (cf. with other f values in fig. 1 of BJK).

3 THE SCALING RELATIONS AT HIGH z

3.1 TF relation

3.1.1 TF scatter for a fixed mass

Fig. 2 shows predictions for our Model A and high-Ω_b model at $z = 3$. At this z, the low-z_f model fails to form discs. To understand

[1] The assumptions of an isothermal profile and effectively instantaneous disc formation constitute a great oversimplification. BJK explore the impact of these assumptions and conclude that, while severe, they do not bear a strong impact on the predicted scaling relations explored here. The halo profile employed here serves as an excellent approximation to a suite of truncated-profile models everywhere except in the core. This discrepancy, however, has little impact on the flat part of the rotation curve with which we are concerned, or on the stellar populations. The most significant effect is an uncertainty in the normalization of the mass–circular velocity relation, but BJK find that this serves primarily only to slide galaxies along the predicted relations, resulting in little or no net change. A complete description of galaxy formation would of course require more detailed modelling of the halo, and halo–disc interactions (e.g. Avila-Reese et al. 1998; Mo et al. 1998; Somerville & Primack 1999; van den Bosch 2000; Firmani & Avila-Reese 2000).

[2] We note that bulges, however, may be present at high z.

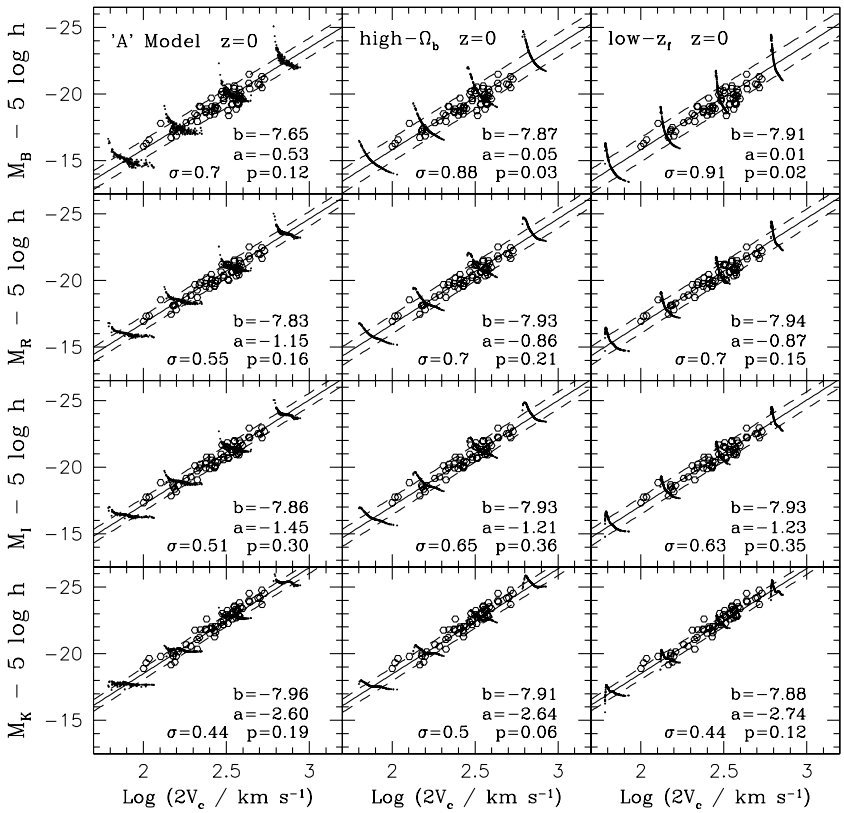

Figure 1. Predicted *B*-, *R*-, *I*- and *K*-band TF relations at $z = 0$ for the A model, high-Ω_b model, and low-z_f model. The scattered dots show the results for fixed masses of 10^{10}, 10^{11}, 10^{12} and $10^{13}\,M_\odot$. The solid lines are the best-fitting TF relations, with zero points and slopes given by a and b, respectively, while the dashed lines show the 1σ scatter, denoted in each plot by σ.

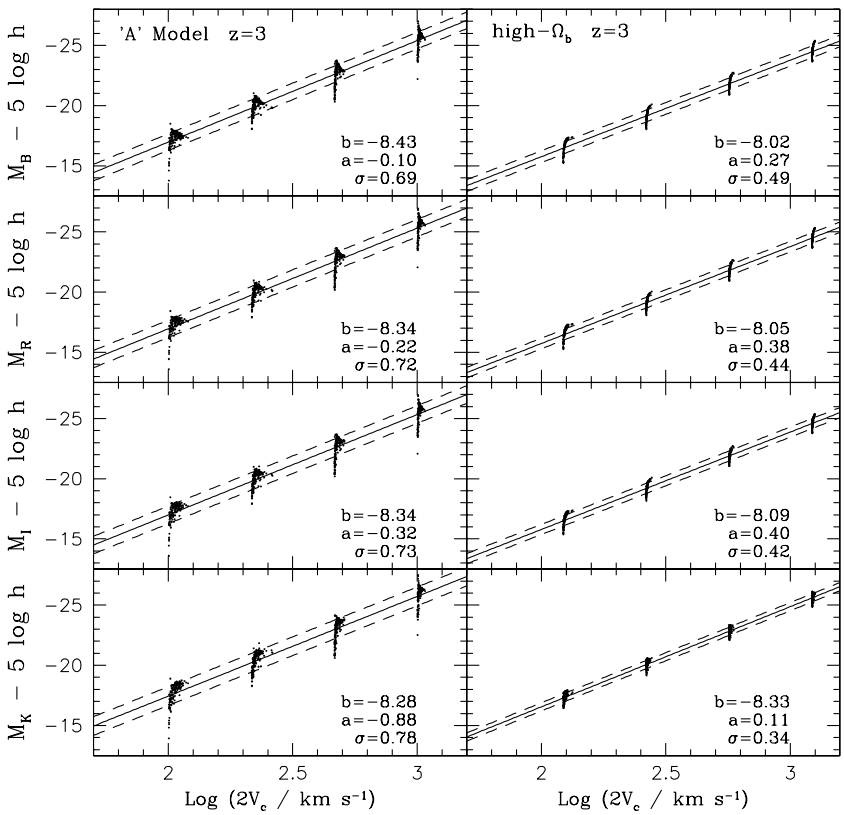

Figure 2. TF predictions of Model A and the high-Ω_b model at $z = 3$. The low-z_f model predicts essentially no discs to have formed at $z = 3$ at these scales.

some of the physical mechanisms at work, we first focus on the scatter for galaxies of a fixed mass (as opposed to the overall scatter), looking specifically at Model A, because it is the most plausible. In the left-hand panels we see that, at *all* wavelengths, the points for a given mass scatter in a nearly vertical direction in contrast to the more horizontal scatter in the $z = 0$ results (see fig. 13 in BJK), particularly in redder bands. For $z = 0$, the TF scatter was seen to arise primarily from the spread in z_f, with the earliest-forming objects of a fixed mass having higher circular velocities. This is because for an evolved galaxy that has converted most of its gas to stars, the light from giants serves as a faithful tracer of the total mass, regardless of the precise age of the galaxy. As one goes either to higher masses in a given waveband, or to bluer bands at a fixed mass, the scatter in the local TF relation for a fixed mass does begin to curve upward (i.e. later-forming discs appear brighter) to form a 'magnitude peak,' because in both cases one becomes increasingly biased towards younger, brighter systems.

At $z = 3$, the scatter still owes mainly to the spread in z_f, and Fig. 2 still indicates that at $z = 3$ the very earliest-forming objects do possess somewhat higher circular velocities for a given mass. (Note, in the left panels, the 'peak' of points formed at the high-V_c end of the four scatter plots for the different masses.) The galaxies that populate the TF relation at $z \gtrsim 3$, however, are the small minority that constitute the exponentially decaying high-z tail of the adopted z_f distribution (fig. 1 of BJK). Thus, the formation of these haloes spans a very short epoch, so that haloes of a given mass will have roughly the same V_c, resulting in the tight horizontal scatter for each mass. The large vertical scatter arises from the fact that, though these galaxies will eventually form the lower envelope of the present-day TF relation comprising the oldest and (in bluer bands) faintest objects of a given mass, at $z = 3$ even the least massive of these galaxies are typically no older than a few 10^9 yr, and the more massive systems are younger still. Thus, systems on the 'young' side of the magnitude peak have formed so close to the epoch of observation that, given their high gas fractions and SFRs, even a small increase in their age results in a substantial increase in their stellar luminosity, at any wavelength.

At high z, discs with circular velocities 200–500 km s^{-1} (masses $\sim 10^{13}$ M$_\odot$) correspond to rare fluctuations. Still, at these z, one does expect to find several such objects within the horizon in a ΛCDM cosmogony, and because these will be the brightest objects in the sample, we include them in the discussion here. We also reiterate that the discs which form at $z \gtrsim 3$ are not the dominant population of discs at $z = 0$, as most discs at $z = 0$ probably formed at $0.5 \lesssim z \lesssim 2$ (see e.g. BJK). Discs forming at higher z will delineate the lower envelope of the TF relation at $z = 0$; for a given mass, these older, higher-V_c systems will be fainter as they will be the first to run out of fuel.

3.1.2 *Overall TF relation*

The trend seen by BJK of steeper TF slopes and fainter zero-points in going from $z = 0$ to $z = 1$ is seen to continue here out to $z = 3$. Specifically, in the B band, the $z = 3$ TF relation goes from ∼2 mag brighter than its local counterpart at $\log 2V_c = 3$ to less than 1 mag brighter at $\log 2V_c = 1.7$. In K, the high-z prediction is comparable to the local prediction at $\log 2V_c = 3.0$, and about 1 mag fainter at $\log 2V_c = 1.7$. This is actually counter to the trend one might expect based on dynamical arguments, as for a fixed mass-to-light ratio, higher values of V_c at higher z should lead to shallower TF slopes. In our models however, the significant luminosity evolution, seen at all wavelengths, is actually seen to be the dominant effect. The key lies in understanding the relative SF efficiency in these systems. For fixed V_c, higher-mass haloes at high z will be younger, smaller and have lower λ than haloes today. In these massive systems, most of the SF activity takes place at very early times and falls of rapidly thereafter (see fig. 7 of Heavens & Jimenez 1999). By contrast, smaller-mass haloes have lower SF efficiencies at early times and thus build up their stellar populations more gradually [see also fig. 1 of Jimenez et al. (1998), and note the fact that in our model the surface density depends on the mass of the disc (Heavens & Jimenez 1999)]. Therefore, looking back to such early stages in their lifetimes, haloes of all sizes will still contain large amounts of unprocessed gas, but smaller-mass haloes will have relatively higher gas fractions. This makes them proportionately dimmer than their present-day counterparts, as compared to higher-mass haloes, and thus results in a steeper TF slope.

The *overall* Model A B-band scatter in the high-z TF relation is comparable to that at $z = 0$. In K, however, the scatter at $z = 3$ has increased by a factor of two. Moreover, the variation in the TF scatter among different wavebands is not as great at high z as was seen in the local case. This is because (i) discs at $z > 3$ are likely to be in a starburst-dominated phase as there is very little cosmological time for even single stellar populations to decay; (ii) at such early times the spread in mass of gas turned into stars is very large for different z_f and λ (see equation 7 of Heavens & Jimenez 1999). Therefore, it seems natural that all bands reflect the maximum possible spread. By contrast, there is little change in TF scatter from $z = 0$ to $z = 1$, as the majority of galaxies are sufficiently evolved by $z = 1$ (figs 13 and 14 in BJK). Furthermore, the scatter obtained here should be considered as an upper limit, because in practice magnitude-limited surveys may not detect arbitrarily young, and therefore faint, objects, particularly at lower masses.[3] However, different realizations of a given model can generally produce results that vary by ≲0.1 mag in the TF scatter. Given the simplifying assumptions of the model, particularly as regarding the assumed mass-circular velocity relation, closer attention should be paid to the overall magnitudes of and relative differences between the slopes, normalizations and scatters, rather than their precise values.

3.1.3 *Spin–peak-height* (ν–λ) *anticorrelation*

Several authors have investigated the impact of the distribution of halo spins of the predicted TF relation (Heavens & Jimenez 1999; Firmani & Avila-Reese 2000). In BJK, we also noted the slight reduction in TF scatter at $z = 0$ in Model A arising from the existence of a possible weak anticorrelation of λ with ν, and thus with z_f. This reduction in TF scatter was only about 0.15 mag in B and 0.05 mag in K for Model A, and a lesser or no effect was seen in some other possibly viable models. To investigate the effect of the joint λ–ν distribution, we re-ran the models in Fig. 2 with $\lambda = 0.05$ for all haloes. This produces TF predictions with shallower slopes and brighter zero-points. This is a result of the fact that the $\lambda = 0.05$ value is higher (lower) than the full model would

[3] Our models employ a minimum time step of 10^7 yr – corresponding to the time-scale for giant molecular cloud destruction (e.g. Jimenez et al. 2000) – that effectively dictates the faintest objects at a given mass, and therefore the maximum possible scatter.

typically assign to high-mass (lower-mass) galaxies, which thus become correspondingly fainter (brighter) in the fixed-λ model. More interestingly, using a fixed λ at high z *reduced* the overall TF scatter by about 0.2 mag in all bands at $z = 3$, as compared with using the joint distribution in λ and z_f. This is in direct contrast to the $z = 0$ case, where a fixed λ produced a comparable or larger scatter, as described above. This can be understood in terms of the vertical nature of the TF scatter for a fixed mass at high z. In this case, higher-λ systems are still fainter, but their lower z_f (already confined to only a narrow range) can only further scatter them to lower luminosities, not to lower V_c as in the local case, thereby increasing the scatter. This suggests that the TF scatter at high z could be used to gauge the strength of any actual λ–z_f anticorrelation.

3.2 The surface-brightness–magnitude relation

Fig. 3 shows the surface-brightness–magnitude relation at $z = 0.4$ and $z = 3$ for Model A and the high-Ω_b model, The dots are from 2dF (Driver & Cross 2000), and the open triangles from the Hubble Deep Field (HDF) (Driver 1999); the latter have $z \simeq 0.4$. As our model does not include a bulge component, the predicted μ may underestimate observed values if the disc and bulge components cannot be resolved.

As was seen in the case of the TF relation, evolution of the stellar populations with z plays a strong role, here yielding a steeper μ–M relation than predicted by simple dynamical arguments (e.g. $\Sigma_0 \propto M_{\rm d}^{1/3}$). For Model A, however, the slope of the relation at $z = 3$ is slightly shallower than the local relation, with μ nearly identical to the low-z case for $M_B - 5\log h > -16$ and fainter by about 1 mag for $M_B - 5\log h = -24$. Thus, at these scales, the trend towards higher luminosities and smaller disc scalelengths is offset by cosmological μ dimming. A more drastic contrast is seen in the high-Ω_b model, where the predicted μ at the bright end varies by almost 4 mag. This owes largely to substantial brightening that occurs at late times as the higher baryon fraction is converted into starlight.

For both models, we find that the scatter at $z \geq 3$ is much tighter than for the local case because the spread in the radii of discs at $z > 3$ is smaller than at low z. For example, at $z \sim 0$, disc sizes span a range roughly between 1 and 100 kpc, while at $z \sim 3$ they range only from about 0.5 to 15 kpc in size. On the other hand, the respective spreads in M differ by no more than a factor of 2. The small spread in the relation then reflects the small spread in disc sizes predicted in our adopted structure-formation scenario. Thus, it will be interesting to learn whether this narrow spread is in fact observed at high z. If a much wider spread is observed, this might indicate that either discs at $z > 3$ are more substantially affected by merger activity or that they are simply larger; i.e. the spread in sizes predicted by our simple isothermal spherical-collapse model with angular momentum conservation is simply too narrow. Note that the μ predictions in general are more sensitive to assumptions regarding λ than are TF predictions, thus providing a strong complementary constraint on this aspect of the model.

3.3 Addressing possible degeneracies

We now address how high-z predictions can be used to distinguish among galactosynthesis models that are degenerate at $z = 0$. The right-hand panels of Fig. 2 show TF predictions for the high-Ω_b model. At these mass scales, the low-z_f model predicts essentially no discs (and thus no TF relation) to be present at $z = 3$, certainly a drastically different prediction than that of the other models, despite their close agreement at $z = 0$.

The precise slopes and zero-points for Model A and the high-Ω_b models differ more appreciably than in the $z = 0$ case, with the latter model yielding predictions that are significantly fainter at these scales. This owes both to the different normalizations of the fluctuation spectrum in the two models and to the fact that the lower SF efficiency in the high-Ω_b model results in fainter discs at early times. More importantly, the predicted TF scatter in the high-Ω_b model is substantially less than that of Model A. This is because (i) a higher value of Ω_0 implies a narrower age range for discs forming at $z \geq 3$ and (ii) the excess scatter caused by a spread in λ,

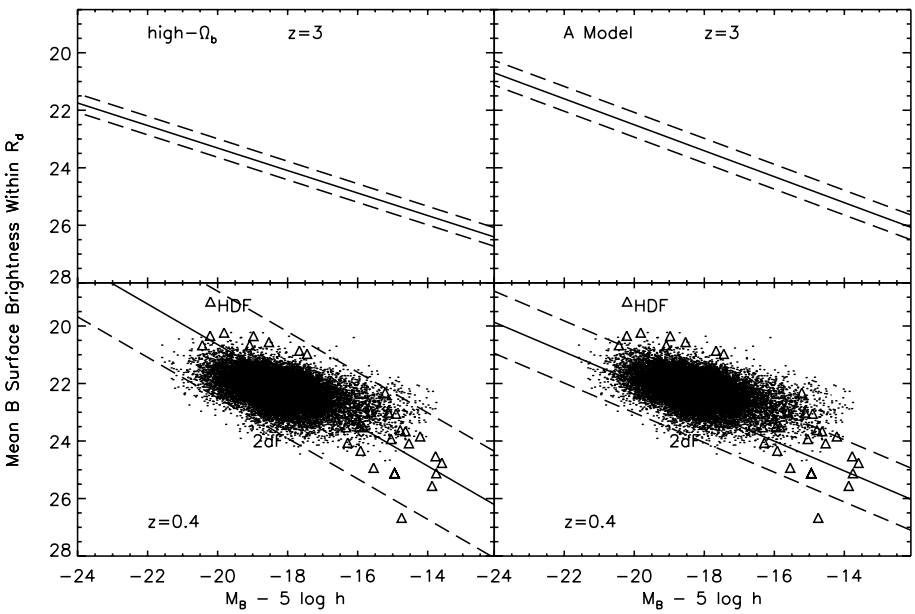

Figure 3. Predicted surface-brightness–magnitude relation for disc galaxies at $z = 0.4$ and $z = 3$ for Model A and the high-Ω_b model. The solid lines are the best-fitting results with a 1σ scatter given by the dashed lines. Note that our model does not include a bulge component.

and additionally by the λ–z_f anticorrelation described above, is excluded in this model.

Alternatively, one could envision a high-z_f model in which discs were somehow brightened at later times, perhaps through late infall of fresh gas. In this case, there might be galaxies that are reasonably evolved, even at these high z, so then many galaxies would be found on the old side of the magnitude peak. Thus the TF scatter for a fixed mass for such objects would more closely resemble that of Fig. 1, rather than the more vertically oriented scatter of Fig. 2, and presumably also lead to a smaller overall TF scatter. In general, other factors not investigated here, such as merging and supernova feedback, could also imprint their signatures on the evolution of the TF relation. The differences among the high-z predictions explored here for the TF relation and its scatter amount to about 1–2 mag and 0.2–0.4 mag, respectively, so these models should be distinguishable with high significance, given data of the type in Fig. 1. The model predictions for the μ–M relation can also be used to address degeneracies. In Fig. 3, we see that, owing to the large scatter, the two models are difficult to distinguish on the basis of low-z predictions, but the tightness of the predicted relation at higher z, if in fact observed, would make this test another powerful discriminator.

4 DISCUSSION

We have presented high-z predictions for the TF and μ–M relations, which may help to discriminate between different scenarios for galaxy formation. The evolution of the TF relation, and in particular its scatter, which owes to different mechanisms as one looks at different wavebands and/or at different epochs, can probe the spread in halo z_f as well as SF processes in the disc. Specifically, for local observations of evolved systems at redder wavelengths, the scatter essentially decouples from the luminosity axis as the light is tracing the total mass roughly independently of the age of the galaxy. By contrast, observations at high z and/or in bluer bands are more sensitive to the age of the disc, resulting in a scatter that couples more closely to the luminosity axis of the TF relation, decoupling almost entirely from the V_c axis in the case of very young systems at $z = 3$. The predicted μ for a given M are fainter and tighter at high z than at low z.

We reiterate that many of these conclusions are a direct result of the significant luminosity evolution predicted by our models. Strong differences in SF properties, particularly at early times, lead to markedly different predictions than would be expected from simple dynamical arguments which assume fixed mass-to-light ratios; the importance of the SF history of discs in predicting the scaling relations explored here is one of the key results of this work.

Several limiting factors must be considered in confronting the models presented in this paper, which is intended only as a starting point for more sophisticated approaches. Features such as the softening of the dark-matter profile towards the core, the adiabatic contraction of the disc, bulge formation, the possible transfer of angular momentum to the halo, feedback from supernovae, the cooling of hot X-ray gas and the impact of mergers have not been addressed. While these factors undoubtedly play a role in the galaxy formation process, BJK and other authors (Avila-Reese & Firmani 2000; Firmani & Avila-Reese 2000) argue that some or all of these are probably only of secondary importance in determining the global disc properties examined here, though future work will be needed to address these issues in a more detailed fashion.

Furthermore, we implicitly assume passive disc evolution, free of major merging events, and that galaxies in the high-z universe are those in the high-z_f tail of the present-day distribution. BJK showed that Model A predictions at $z = 1$ agreed with a limited data set (Vogt et al. 1997), but these galaxies were selected to resemble local discs. It has so far proven difficult to extract reliable V_c measurements for discs comprising the general SF population at $z = 1$. Recent data seem to suggest that beyond the local universe, 'normal' galaxies actively form stars primarily in their small cores (see e.g. Simard & Pritchet 1998; Rix et al. 1997). Linewidth measurements of SF galaxies at $z = 1$ and $z = 3$ are found to sample effectively only the core dispersion, yielding typical values of roughly $80\,\mathrm{km\,s^{-1}}$ with a scatter of about 20–$30\,\mathrm{km\,s^{-1}}$ over a range of several mag. Unless improved measurements can succeed in sampling the disc at larger radii (or at some other means of tracing the potential), a proper TF relation may not be easily defined.

Progress might be made by focusing on the lower, red envelope of the TF relation, rather than attempting to fill in the TF plane. We find that the locus of the oldest and reddest points in the TF plane generally lie themselves on a well-defined line that serves as the high-z_f envelope to the relation. Samples of these old, red objects might be easier to construct than complete TF samples, which include young, starbursting objects that may have arbitrarily low luminosities falling off on the younger side of the magnitude peak. SIRTF and NGST will have the sensitivity to detect some of the reddest objects in the sky, even out to high z. If so, a comparison of the red envelope formed by these old objects with the predictions, could suffice to constrain many of the key aspects of galactosynthesis models without needing to populate the entire TF plane. Of course, the effects of dust will need to be taken into account too, so that young, dusty systems are distinguished from old galaxies.

ACKNOWLEDGMENTS

We wish to acknowledge C. C. Steidel and K. A. Adelberger for helpful discussions. We also wish to thank the referee, Vladimir A. Avila–Reese, for useful suggestions and comments, specially regarding the M/L ratios of the model. This work was supported by grants NSF-AST-0096023, NSF-AST-9900866, NSF-AST-9618537, NASA NAG5-8506, and DoE DE-FG03-92-ER40701.

REFERENCES

Avila-Reese V., Firmani C., 2000, Rev. Mex. Astron. Astrofis., 36, 23
Avila-Reese V., Firmani C., Hernandez X., 1998, ApJ, 505, 37
Bardeen J. M., Bond J. R., Kaiser N., Szalay A. S., 1986, ApJ, 304, 15
Bottema R., 1996, A&A, 328, 517
Buchalter A., Jimenez R., Kamionkowski M., 2001, MNRAS, 322, 43
Bunn E. F., White M., 1997, ApJ, 480, 6
Catelan P., Theuns T., 1996, MNRAS, 282, 455
Dalcanton J. J., Spergel D. N., Summers F. J., 1997, ApJ, 482, 659
Driver S. P., 1999, ApJ, 526, L69
Driver S. P., Cross N., 2000, ASP Conf. Ser. Vol. 218, Mapping the Hidden Universe: The Universe behind the Milky Way – The Universe in H I. Astron. Soc. Pac., San Francisco, p. 309
Eisenstein D. J., Loeb A., 1996, ApJ, 459, 432
Firmani C., Avila-Reese V., 2000, MNRAS, 315, 457
Heavens A. F., Jimenez R., 1999, MNRAS, 305, 770
Heavens A. F., Peacock J. A., 1988, MNRAS, 232, 339
Jimenez R., Padoan P., Matteucci F., Heavens A. F., 1998, MNRAS, 299, 123

Jimenez R., Padoan P., Dunlop J. S., Bowen D. V., Juvela M., Matteucci F., 2000, ApJ, 532, 152
Kennicutt R. C., 1998, ApJ, 498, 541
Lacey C., Cole S., 1993, MNRAS, 262, 627
Lacey C., Cole S., 1994, MNRAS, 271, 676
McGaugh S. S., De Blok W. J. G., 1997, ApJ, 481, 69
Mo H. J., Mao S., 2000, MNRAS, 318, 163
Mo H. J., Mao S., White S. D. M., 1997, MNRAS, 295, 319
Navarro J. F., Steinmetz M., 2000, ApJ, 538, 477
Rix H., Guhathakurta P., Colless M., Ing K., 1997, MNRAS, 285, 779
Roberts M. S., Haynes M. P., 1994, ARA&A, 32, 115
Simard L., Pritchet C. J., 1998, ApJ, 505, 96
Somerville R. S., Primack J. R., 1999, MNRAS, 310, 1087
Tully R. B., Pierce M. J., Huang J. S., Saunders W., Verheijen M. A. W., Witchalls P. L., 1998, AJ, 115, 2264
van den Bosch F. C., 2000, ApJ, 530, 177
Verheijen M., 1997, PhD thesis
Vogt N. P. et al., 1997, ApJ, 479, L121

This paper has been typeset from a TEX/LATEX file prepared by the author.